ANALYTICAL CALIBRATION PROCEDURES FOR UNDERWATER CAMERAS

J. G. Fryer* and C. S. Fraser
Geodetic Services, Inc.
1511 S. Riverview Drive
Melbourne, Florida 32901

ABSTRACT

The application of two analytical methods, namely self-calibration and the plumb-line technique, for the calibration of underwater cameras is reported. Aspects of these methods are reviewed and results obtained in the calibrations of a Rolleiflex SLX 70mm Reseau camera (with sub-marine housing) and a Nikonos 35mm underwater camera are discussed. The results indicate that with analytical calibration semi-metric and non-metric cameras can be employed for underwater photogrammetric measuring tasks requiring relatively high accuracy.

INTRODUCTION

Geodetic Services, Inc. recently completed a project in which a close-range cine photogrammetric system was developed for measuring the dynamic performance of a projectile under water. Components of this system included eight high-speed 16mm cine cameras, two still cameras, and an automated data mensuration and reduction system which was designed to measure and process up to 500 six-photo photogrammetric networks comprising some 30-40 object points in 24 hours.

Part of the monitoring requirement called for the measurement of about 50 points on the object when it was stationary. The camera selected for this phase was a Rolleiflex SLX Reseau with a 50mm Distagon f-4 lens. To facilitate underwater use of this 70mm semi-metric camera an Aquamarin WKD-SLX/6006 Sub-Marine housing was obtained. As a backup to the Rolleiflex a Nikonos V 35mm underwater camera with a 28mm Nikkor-UW f-3.5 lens was added to the system. Figure 1 shows each camera and the underwater housing.

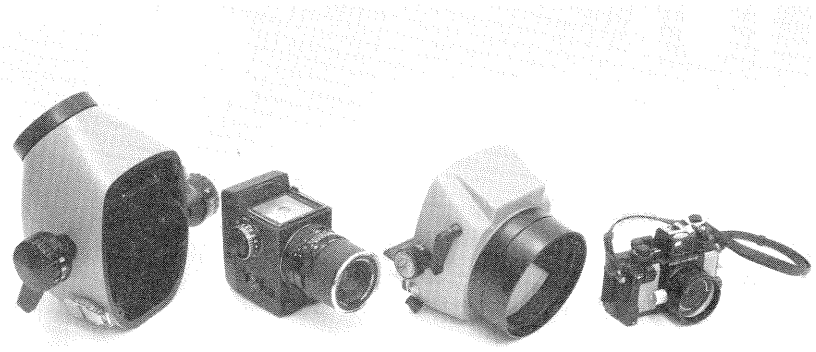

Figure 1: Rolleiflex SLX Reseau camera, Aquamarin WKD-SLX/6006 housing and Nikonos V underwater camera.

* On sabbatical leave from the Dept. of Civil Engineering & Surveying, University of Newcastle, Newcastle, New South Wales, Australia 2308.

For the underwater static-state measurements of the object, which occupied a volume of 3m by 3m by 2m (high), the Rolleiflex (or Nikonos where necessary) was to be used at a depth of close to 20m. Photogrammetric networks comprising four or five camera stations, with two photos per station, were required to yield the specified point positioning accuracy of one millimeter. An imaging scale of 1:60, or about 4.5m away from the object in the case of the Rolleiflex, was adopted for the photography. In addition to the underwater measurements, target locations on the object were also required to be measured prior to submersion in order to detect any structural deformation due to pressure changes.

To familiarize personnel with the operation of the Rolleiflex and Nikonos cameras, and to check the data reduction schedule, a series of camera calibration tests in air and in water were performed. In air, the camera calibrations consisted of plumb-line photography with subsequent reduction for radial and decentering distortion. Underwater, plumb-line photography and self-calibrations for all parameters of distortion and interior orientation were made using a test fixture at about one-third scale (for ease and convenience of handling) of the real test equipment.

In this paper the camera calibration procedures adopted for the Rolleiflex and Nikonos cameras are discussed and the calibration results presented. The scope of the paper does not extend to a discussion of the calibration procedure adopted for the 16mm movie cameras, though the approach employed was very similar to that used for the self-calibrations of the still cameras. Moreover, the mathematical foundations of the analytical plumb-line and self-calibration techniques are not covered in the present paper and readers desirous of a more complete mathematical treatment are referred to the photogrammetric literature; notably the proceedings from ISP Commission V meetings at Hamburg, York and Rio de Janeiro (ISP, 1980, 1982, 1984) in the case of self-calibration, and to Brown (1971) and Fryer and Brown (1986) for details of the plumb-line method. A more detailed version of the contents described here can be found in Fryer and Fraser (1986).

ANALYTICAL CALIBRATION METHODS

Self-Calibration

Under the self-calibration approach the photogrammetric system (principally the camera) is calibrated as part of the analytical restitution process. For a particular camera focus setting, both the elements of interior orientation and the distortion characteristics of the lens are mathematically modelled. The three interior orientation parameters are c, the principal distance, and x_p and y_p, the coordinates of the principal point. Lens distortion can be described in terms of its two components, symmetric radial and decentering distortion. Radial distortion is most often modelled by the well-known odd-order polynomial expression

$$D(r) = K_1 r^3 + K_2 r^5 + K_3 r^7 \qquad (1)$$

where r is the radial distance from the principal point, and K_1, K_2 and K_3 are termed the coefficients of radial distortion. In describing the decentering distortion it is necessary to recover both the decentering distortion profile function and the phase angle between the x image coordinate axis and the axis of maximum tangential distortion. The profile function is defined as

$$P(r) = (P_1^2 + P_2^2)^{\frac{1}{2}} r^2 \qquad (2)$$

where P_1 and P_2 are the coefficients of decentering distortion. The phase angle can be determined from P_1 and P_2 through the expression $\phi_0 = \arctan(P_1/P_2)$.

Both radial and decentering distortion vary with focussing of the lens in a predictable manner, and for any particular focus there is a variation of the

distortion for points in planes at different distances from the camera. For close-range photogrammetry a knowledge of the distortion functions at two distinct focus settings is required to accurately reduce observed image point coordinates to their 'true' positions.

In applying self-calibration, an additional parameter model must first be defined. This model may comprise physically interpretable parameters (such as distortion coefficients and interior orientation elements), coefficients of polynomial error functions in x and y (including orthogonal polynomials), or combinations of both. For the reported investigation the following additional parameter model was selected:

$$\begin{aligned} \Delta x &= -x_p + \left(\frac{-\bar{x}}{c}\right)dc + \bar{x}(K_1 r^2 + K_2 r^4 + K_3 r^6) + P_1(r^2 + 2\bar{x}^2) + 2P_2\bar{x}\bar{y} \\ \Delta y &= -y_p + \left(\frac{-\bar{y}}{c}\right)dc + \bar{y}(K_1 r^2 + K_2 r^4 + K_3 r^6) + P_2(r^2 + 2\bar{y}^2) + 2P_1\bar{x}\bar{y} \end{aligned} \qquad (3)$$

where Δx and Δy are the corrections to image coordinates and dc is the correction to the principal distance c. The image coordinates $\bar{x}$ and $\bar{y}$ are with respect to the principal point, i.e.,

$$\begin{aligned} \bar{x} &= x - x_p \\ \bar{y} &= y - y_p \end{aligned} \qquad (4)$$

where x and y are the measured image coordinates (with origin at the fiducial center). The model given in Equation 3 has been referred to as a 'physical' self-calibration model in that it contains only the traditional distortion coefficients (K_1, K_2, K_3, P_1 and P_2) and the elements x_p, y_p and c of interior orientation. Based on the results of previous self-calibration investigations of semi-metric and non-metric cameras it was decided not to augment the model with empirical additional parameters to describe film deformation and unflatness effects since such an approach has been found in most cases to yield no improvement in accuracy over the 'physical' model (e.g. Fraser, 1984).

Self-calibration enables the application of semi-metric (for example, the Rolleiflex SLX Reseau) and non-metric, 'amateur' cameras (the Nikonos V) in photogrammetric surveys which demand moderately high accuracy. Accuracies exceeding one part in 5000 (and up to 1 part in 25000) of the object's principal dimension are now routinely possible with a combination of non-photogrammetric cameras and the procedure of self-calibration.

Plumb-line Calibration

The analytical plumb-line technique only produces values for the parameters of radial and decentering distortion. It is based on the projective principle that, in the absence of distortion, the photographic image of a straight line is itself a straight line image. Departures from linearity are attributed to distortion. As is indicated in Equation 3, distortion gives rise to image shifts which can be modelled in terms of correction components to photographic coordinates as:

$$\begin{aligned} \Delta x &= \bar{x}(K_1 r^2 + K_2 r^4 + K_3 r^6) + P_1(r^2 + 2\bar{x}^2) + 2P_2\bar{x}\bar{y} \\ \Delta y &= \bar{y}(K_1 r^2 + K_2 r^4 + K_3 r^6) + P_2(r^2 + 2\bar{y}^2) + 2P_1\bar{x}\bar{y} \end{aligned} \qquad (5)$$

The observation equations for the plumb-line method (Brown, 1971) contain the parameters K_1, K_2, K_3, P_1 and P_2. Although the principal point coordinates x_p and y_p also appear implicitly in Equation 5, they can only be recovered with a reasonable degree of confidence when the distortion is exceedingly large, as with fish-eye lenses. The principal distance c for the focus setting used cannot be determined using the analytical plumb-line method.

The plumb-line technique derives its name from the thin plumb-lines that were initially strung in a plane as the object lines. More recently, considerable

success has been reported (Fryer and Brown, 1986) using relatively thick (1.25mm diameter) white nylon cord which is stretched taut and reasonably vertical by means of turnbuckles. The thicker cord provides an excellent target for automatic video-scanning monocomparators with line-following capabilities, such as AutoSet-1 (ibid).

A Comparison of Methods

The plumb-line and self-calibration techniques share few common features. One, however, is that neither requires any object space control, other than the constraint that the plumb-lines are indeed straight. With self-calibration a 'strong' photogrammetric network displaying specific geometric features (e.g. a convergent configuration with a diversity of camera roll angles between exposure stations) is required. Invariably, a network of some four to eight photos is warranted. In the plumb-line method, on the other hand, only one photo of the array of plumb-lines is required. If film flatness and deformation can be contained within acceptable limits by a reseau, or vacuum platen, there is no theoretical objection to rolling the camera through 90° and taking a second image of 'horizontal' lines on a separate photograph. Both sets of data can then be merged for a simultaneous solution for the parameters of radial and decentering distortion.

The main benefit of the plumb-line procedure in comparison to self-calibration is that it is faster when an automatic comparator is employed. The obvious shortcoming of the method, on the other hand, is that it only affords the recovery of distortion parameters and not the elements of interior orientation. A secondary advantage of the plumb-line technique is the ease with which distortion can be calibrated at different focus settings. If the plumb-line method is applied for two distinct principal distances, say photographic scales of 1:20 and 1:60 for the case of a non-metric camera with a 50mm lens, then the parameters of distortion at any other required object distance may be computed using Brown's extension of Magill's formula (see Brown, 1971 and Fryer and Brown, 1986).

CALIBRATION APPLICATIONS

Field Procedures

For the in-air plumb-line calibration of the Rolleiflex an array of some 20 vertical lines of nylon cord was photographed at three focus settings. The three imaging scales adopted were 1:20, 1:40 and 1:60. For the 20X magnification, seven plumb-lines were exposed, and for the 40X and 60X magnification 14 of the 20 imaged plumb-lines were selected for measurement. To check the optical properties in air of the 12.5mm thick plane glass port of the marine housing, the plumb-line range was again photographed at the same three scales with the camera in the housing.

In the underwater calibrations the portable test field shown in Figure 2 served as a target range. A total of 98 targets were affixed to the aluminum frame and to the nine nylon cords strung between the frame's sides. The framework was by no means dimensionally stable, but that was of little consequence as it did not deform in shape during the few minutes in which the photography was taken.

An eight station photogrammetric network with convergent geometry was used for the self-calibrations. At each of four positions, approximately 2.5m from the target field, two photographs at a scale of about 1:35 were taken with the Rolleiflex. The camera was rolled through 90° between exposures. A similar geometry was adopted for the Nikonos photography, however the camera to object distance was reduced to 1.9m resulting in a mean imaging scale of 1:50. In this manner, three principal geometric requirements for obtaining a strong self-calibration of the interior orientation parameters were met. These were the adoption of a convergent imaging configuration, the use of a three-dimensional target array (which is not strictly necessary if the photography is highly convergent), and the provision of a diversity of camera roll angles.

Due both to the size of the frame on which the nylon cord was strung and the depth of the swimming pool used for the tests, photography for the underwater plumb-line calibrations could only be performed at scales of 1:10 and 1:20 with the Rolleiflex, and 1:20 and 1:40 with the Nikonos. Refraction at the water/lens interface causes the focal length of a camera immersed in water to appear to increase by a factor of 1.34, a common value for the refractive index of water. A focal length value closer to 70mm than 50mm must therefore be assumed when the Distagon lens is used in water. The corresponding increase in the 28mm Nikkor-UW lens is about 10mm, bringing the focal length to a nominal value of 38mm. When using the two cameras underwater the lens must be pre-focussed to 0.75 of the true distance to allow for the refraction effect.

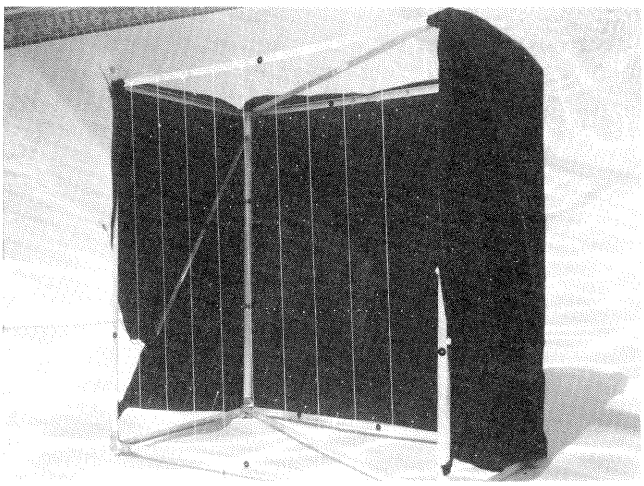

Figure 2: Test frame used for underwater calibrations.

Ektachrome color transparency film, ASA 200, was employed for all tests as this film had been chosen for the actual project. In each frame for the plumb-line calibrations some 250-300 points were measured. The photographs of the underwater plumb-lines were more difficult to read than those taken in air due to water clarity and lighting problems. Consequently, the RMS values of the x,y residuals from the underwater plumb-line calibrations were larger than those in the in-air calibrations.

Results of Plumb-Line Calibrations

The Gaussian radial distortion profiles resulting from the in-air calibrations of the Rolleiflex 50mm Distagon f-4 lens are shown in Figure 3. A "balancing" of these distortion curves was performed so that the mean distortion value out to a radial distance of 30mm was zero (see plots in Fryer and Fraser, 1986). The resulting balanced distortion curves were very similar in character to one shown in Wester-Ebbinghaus (1983). The considerable radial distortion effects of the plane glass port of the Aquamarin housing are illustrated by the distortion profiles in Figure 4. In the computation of each distortion profile, the RMS value of image coordinate residuals from the 300 or so observations in the least-squares plumb-line calibration adjustment was close to 2 μm.

Primarily as a result of the poorer imagery obtained in the underwater photography with the Rolleiflex in its Aquamarin housing, the precision of the plumb-line calibrations was marginally poorer underwater than in air. An average RMS value for the underwater plumb-line calibrations was 4 μm. For the radial distortion profile underwater see column (4), Table 1.

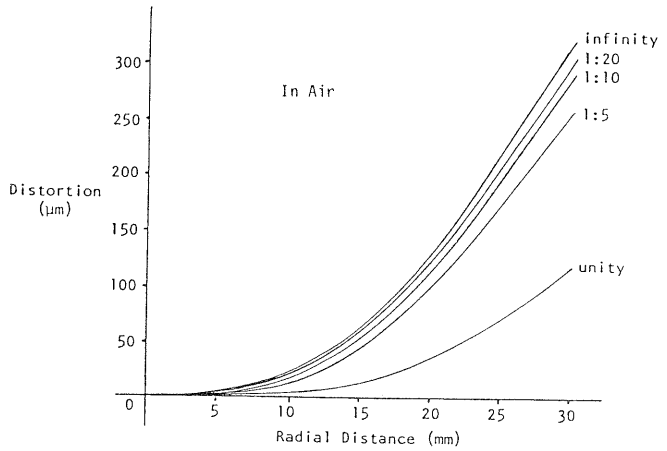

FIGURE 3. Gaussian radial distortion for varying photographic scales. Camera is Rolleiflex SLX Reseau with 50mm Distagon f-4 lens, in air.

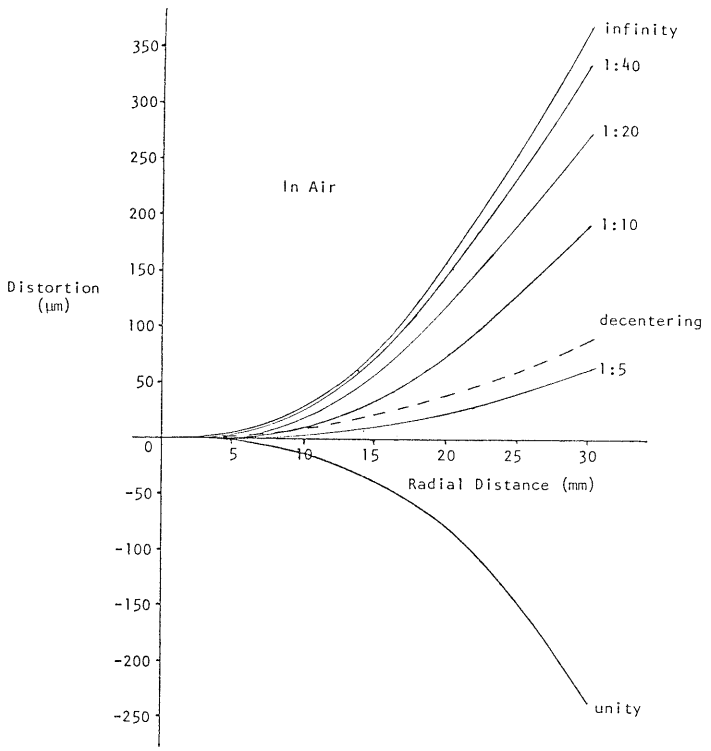

FIGURE 4. Gaussian radial distortion for varying photographic scales. Camera is Rolleiflex SLX Reseau plus Aquamarin WKD-SLX/6006 Sub-Marine Housing in air with 50mm Distagon f-4 Lens. (Compare Figure 3.) Decentering distortion profile shown as dashed line.

Table 1. Comparison of predicted radial distortion for the plane port on an underwater housing with values observed at a scale of 1:20.

RADIAL DISTORTION: Distagon 50mm f-4 Lens, Aquamarin WKD-SLX/6006 Housing.					
r (mm) (1)	Predicted for Plane Window (2)	Observed (Plumb-lines) In Air (3)	Observed (Plumb-lines) In Water (4)	Observed Plane Window Distortion (5) = (3) - (4)	Differences Predicted-Observed (6) = (2) - (5)
5	+8.7 µm	+2.2 µm	-6.5 µm	+8.7 µm	0.0 µm
10	+69.4	+17.1	-52.7	69.8	-0.4
15	+233.2	+53.8	-180.1	233.9	-0.7
20	+549.6	+115.2	-434.3	549.5	+0.1
25	+1066.7	+194.5	-869.1	1063.6	+3.1
30	+1824.9	+273.2	-1551.0	1824.2	+0.7

The total effect of radial distortion due to the water/plane port interface can be obtained by a subtraction of the observed radial distortions in air from those in water, using the common scale of 1:20. As a totally independent check on the plumb-line calibrations, the radial distortion effect δr of water on a plane port can be predicted using the formula (McNeil, 1972)

$$\delta r = \left(\frac{\cos \phi}{\cos \phi''} - 1 \right) r \qquad (6)$$

in which ϕ is the angle from the optical axis to an underwater target, ϕ'' is the corresponding angle inside the camera to that target's image and r is the induced radial distortion.

The predicted values for the radial distortion are shown in column (2) of Table 1 and the difference between the predicted and observed values are in column (6). The remarkably good agreement, an RMS discrepancy value of 1.4 µm over a range of values up to 1800 µm, is an indication of the effectiveness of the analytical plumb-line method for determining radial distortion.

The combination of the underwater housing and the Rolleiflex camera produced a relatively high value of 91 µm for the decentering distortion profile P(r) at a radial distance of 30mm, as shown in Figure 4. Large values of decentering distortion make it imperative that formulae be employed in the self-calibrating bundle adjustments which accommodate variations in decentering distortion both for focus setting and for variation within the photographic field employed (see Fryer and Brown, 1986).

The Gaussian radial distortion profiles from the underwater plumb-line calibration of the 28mm Nikkor-UW f-3.5 lens are shown in Figure 5, and Figure 6 shows an equivalent set of balanced curves such that the mean value of the distortion is zero out to a radial distance of 20mm. The corresponding increments to the 38.6mm underwater principal distance are also presented. Figure 6 compares nicely with the radial distortion curve produced by Höhle (1971) for this type of lens. The level of the precision of recovery of the radial and decentering

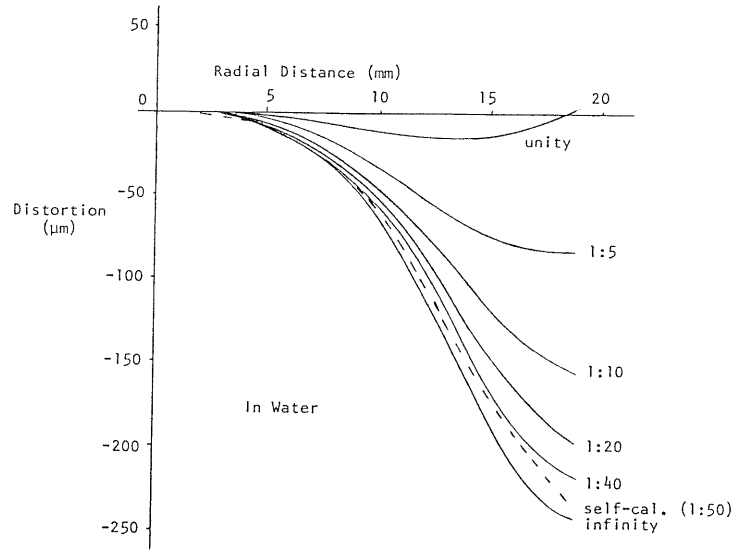

FIGURE 5. Gaussian radial distortion for varying photographic scales. Camera is Nikonos V with 28mm Nikkor-UW f-3.5 lens. Underwater profile from self-calibration indicated at approximate scale of 1:50.

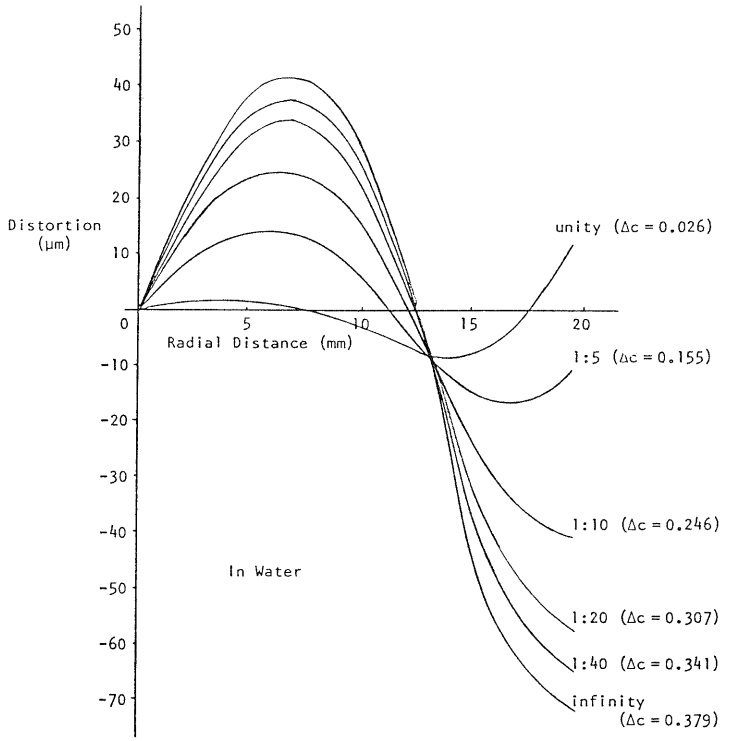

FIGURE 6. Balanced radial distortion for a radial distance of 20mm. Camera is Nikonos V with 28mm Nikkor f-3.5 lens. Variation of (underwater) 38.6mm principal distance indicated by c values (mm).

distortion parameters in the Nikonos calibrations was similar to that achieved with the Rolleiflex. An RMS value of residuals of just over 2 μm was again obtained.

The profile of the decentering distortion for the Nikonos produced a very low value of 3 μm for r = 20mm. Since this distortion is a reflection of how precisely the lens elements have been centered, one can only conclude that the sample tested was well made!

Results of Self-Calibrations

The eight-station self-calibration adjustment for the Rolleiflex yielded standard errors (one-sigma) for the interior orientation parameters x_p, y_p and c of just under 0.02mm. The principal distance was found to be 70.50mm, which corresponds to an in-air value of 52.60mm for the nominally 50mm lens focussed under water at 1.8m (equivalent to a 2.5m in-air focus). The agreement between the values for the radial distortion parameters from the self-calibration and the analytical plumb-line method was excellent. Indeed, at a radial distance of 30mm (a practical working limit for the Rolleiflex), the Gaussian radial distortion profiles differed by only 4.5 μm (in over 1500 μm). Over the remainder of the profile the discrepancy averaged 2.5 μm which was well within the one-sigma error bound on each profile.

For the decentering distortion profile the maximum discrepancy between the two determinations was only 2.1 μm at r = 30mm where P(r) reached a value of 91 μm. The average difference was about 1 μm which is again well within the one-sigma error bound. Separate figures showing the distortion curves from the self-calibration have not been presented as they are, for all practical purposes, the same as plumb-line calibration profiles.

To assess the photogrammetric positioning accuracy of the Rolleiflex SLX Reseau in a close-range underwater environment, one must examine the computed standard errors of the XYZ coordinates of object points. From the covariance matrix $\underline{C}$ of coordinates for all object points it is possible to compute a 'mean' standard error value $\bar{\sigma}_c$ for the XYZ coordinates:

$$\bar{\sigma}_c = (\mathrm{tr}\ \underline{C}_x/3n)^{\frac{1}{2}} \qquad (7)$$

where tr indicates the trace operator and n is the number of points. By considering each coordinate axis separately, one can also use equations of the type above to compute the 'mean' axial standard errors $\bar{\sigma}_X$, $\bar{\sigma}_Y$ and $\bar{\sigma}_Z$.

For the array of 98 targeted points, the adjustment for the underwater self-calibration yielded the following standard error estimates: $\bar{\sigma}_c$ = 0.20mm, $\bar{\sigma}_x$ = 0.18mm, $\bar{\sigma}_y$ = 0.26 mm and $\bar{\sigma}_z$ = 0.15mm (the Y axis was oriented towards the camera stations). The value of $\bar{\sigma}_c$ corresponds to a proportional accuracy of 1 part in 8000 of the object field dimension. This is a much higher level of precision than that normally anticipated for underwater photogrammetric measurement (e.g. Adams, 1982).

In the self-calibrating bundle adjustment of the Nikonos V the interior orientation elements x_p, y_p and c were recovered to a one-sigma precision of 0.04mm. The nominal in-air focal length of 28mm had a corresponding underwater principal distance of 38.6mm for the 1.4m focus setting. To provide a common image frame reference for the non-metric Nikonos, two fiducial marks were added by filing notches into the sides of the film frame.

The self-calibration adjustment exhibited 960 degrees of freedom and an RMS value of image coordinate residuals of 4.4 μm was obtained. This value represented a 1.3μm improvement in closure over the Rolleiflex self-calibration, and the improvement is attributed to the more favorable photographic conditions which prevailed during the Nikonos test. As a consequence, markedly better image quality was obtained with the 35mm camera.

As with the Rolleiflex, the self-calibration of the Nikonos yielded distortion profiles which were in close agreement with those obtained by the plumb-line technique. Over a radial distance of 18mm the average discrepancy in the radial distortion profile was 2 um, although the difference did approach 6 um at r = 10mm. Figure 5 shows the radial distortion profile from the self-calibration as a dashed line amongst the plumb-line distortion curves.

On comparing the decentering distortion profiles from the plumb-line calibration and the self-calibrating bundle adjustment a sizable discrepancy was found. At a radial distance of 18mm the P(r) value from the plumb-line calibration was 3 um, versus a value of 37 um from the bundle adjustment. In searching for an explanation for this difference it was noted that the correlation between the principal point coordinates x_p, y_p and the decentering distortion parameters P_1, P_2 was exceedingly high, a feature which is frequently observed in close-range camera self-calibration.

To verify that the discrepancy between the plumb-line and self-calibration decentering profiles was due to projective compensation between additional parameters a further bundle adjustment run was made. In this, P_1 and P_2 were tightly constrained to the values computed from the plumb-line calibration. The result was that x_p and y_p changed significantly, in fact by 0.14 and 0.33mm respectively. The RMS value of the residuals, however, was only inflated by 0.06 um, and the change to the computed XYZ object point coordinates was insignificant for all practical purposes.

While it may be disturbing to readers who are used to the notion of 'fixed' camera calibration parameters, the variations in the self-calibrated values of x_p, y_p, P_1, and P_2 are of little consequence; the important consideration is that the photogrammetric positioning accuracy of the object point coordinates is not degraded even though the values of the additional parameters may alter significantly between successive photogrammetric surveys. Only where over- parameterization leads to poor conditioning of the normal equations will the results for the object point coordinates be adversely affected.

A mean positional standard error value of $\bar{\sigma}_c$ = 0.3mm was obtained for the 91 target points in the Nikonos self- calibration adjustment. Expressed as a proportional accuracy, this is equivalent to one part in 5300 of the principal object field dimension. Axial standard error estimates of $\bar{\sigma}_X$ = 0.23mm, $\bar{\sigma}_Y$ = 0.40mm and $\bar{\sigma}_Z$ = 0.20mm were obtained. As with the Rolleiflex network, the positional accuracy obtained with the Nikonos was reasonably high. It must be kept in mind that this underwater camera fits very clearly into the class of non-metric, 'amateur' cameras which are designed with neither a film flattening mechanism nor fiducial marks.

CONCLUDING REMARKS

As far as the authors are aware, results of comparisons between two independent analytical calibration techniques for close-range cameras have not previously been published. Furthermore, the degree of precision obtained in the underwater plumb-line method and self-calibrations of the Rolleiflex and Nikonos cameras appears to be a considerable improvement over the published results of other underwater calibration techniques (see, for example, Adams, 1982; Fryer, 1982; Höhle, 1971; McNeil, 1972; Newton, 1984 and Pollio, 1968).

The combination of rigorous analytical techniques, coupled with observational data sets exhibiting high redundancy has yielded underwater camera calibrations to an accuracy approaching those carried out in air. The results reported in this paper illustrate that with analytical calibration techniques, photogrammetric measurement underwater can be carried out to the relatively high accuracies of better than one part in 5000 using semi-metric and non-metric close-range cameras. The problems of underwater photography, however, especially those relating to image quality, should not be underestimated.

REFERENCES

ADAMS, L.P., 1982, Underwater Analytical Photogrammetry using Nonmetric Cameras, Int. Arch. Photo, 24 (V/1): 12-22.

BROWN, D.C., 1971, Close Range Camera Calibration, Photo. Eng., 37 (8): 855-866.

FRASER, C.S., 1984, Multiple Exposures in Non-Metric Camera Applications, Int. Arch. Photo., 25 (A5): 286-295.

FRYER, J.G., 1982, Underwater 35mm Photogrammetric Applications in Australia, Int. Arch. Photo., York, 24 (V/I): 167-174.

FRYER, J.G. and FRASER, C.S., 1986, On the Calibration of Underwater Cameras. Photogrammetric Record (In Press).

FRYER, J.G. and BROWN, D.C., 1986, Lens Distortion for Close Range Photogrammetry, Photo. Eng. and Remote Sensing, 52 (1): 51-58

HÖHLE, J., 1971, Reconstruction of the Underwater Object, Photo. Eng., 37 (9): 948-954.

Int. Soc. Photo., 1980, Hamburg, Commission V, Proc. reprinted in Int. Arch. Photo., 23 (B5): 853 pages.

Int. Soc. Photo., 1982, York, Commission V, Proc. reprinted in Int. Arch. Photo., 24 (V/I and V/II), 557 pages.

Int. Soc. Photo., 1984, Rio de Janeiro, Commission V, Proc. reprinted in Int. Arch. Photo., 25 (A5): 796 pages.

McNEIL, G.T., 1972, Optical Fundamentals of Underwater Photography, 2nd Ed., Mitchell Camera Corp., Rockville, Maryland, 119 pages.

NEWTON, I., 1984, The Current Status of Underwater Photogrammetry, Int. Arch. of Photo., 25 (A5): 580-589.

POLLIO, J., 1968, Applications of Underwater Photogrammetry, U.S. Naval Oceanographic Office Informal Report 68-52, Washington, 38 pages.

WESTER-EBBINGHAUS, W., 1983, Ein photogrammetrisches System fur Sonderanwendungen, Bildmessung und Luftbildwesen, 3: 118-128.